

Effect of Macroscopic Structure in Iridescent Color of the Peacock Feathers

Shinya YOSHIOKA* and Shuichi KINOSHITA

Graduate School of Frontier Biosciences, Osaka University, Toyonaka, Osaka 560-0043, Japan

**E-mail address: syoshi@mph.phys.sci.osaka-u.ac.jp*

(Received May 16, 2002; Accepted June 3, 2002)

Keywords: Iridescence, Peacock Feather, Structural Color

Abstract. We have performed the structural and optical studies on the iridescent peacock feathers. The periodic structure of the submicron melanin granules has been observed beneath the feather surface and is considered responsible for the optical interference. In addition, the macroscopic structures such as the surface curvature and the configuration of barbules considerably affect the reflection properties. A simple model which takes both the submicron and macroscopic structures into account is proposed to explain the essential part of the iridescence in peacock feathers.

1. Introduction

Coloring in biological world sometimes utilizes not only the light absorption of pigments but also various optical phenomena such as interference, diffraction and scattering of light. The latter coloration is called structural color, because the interaction between light and submicron structure is essential in the phenomena. Peacock feather is one of the most well-known examples for the structural color. The first scientific observation on peacock feather was perhaps made by Newton in the 18th century and he pointed out that the optical interference was related with its iridescence (NEWTON, 1730). In the beginning of the 20th century, MASON (1923a, b) performed the careful observations on many kinds of bird feathers and discussed the similarities of their iridescent color to that of thin films. Later, the electron microscope investigations revealed surprisingly minute structure in the feathers of peacock (DURRER, 1962), the humming birds (GREENWALT, 1960; SCHMIDT and RUSKA, 1962), the pheasant (SCHMIDT and RUSKA, 1962) and the ducks (RUTSCHKE, 1966). In these birds, melanin granules form the submicron periodic structure with the periodicity comparable with the wavelength of visible light and are thought to be the origin of optical interference. The spongy medullary structure responsible for the structural color was also found in many kinds of birds and analyzed with 2D Fourier transformation (AUBER, 1957; DYCK, 1971; PRUM *et al.*, 1998, 1999).

In general, the interaction of light with actual submicron structures is difficult to treat strictly, because the complex boundary conditions should be imposed to Maxwell's

equations. Thus, the reflection properties of the structure in iridescent feathers have been often discussed with the thin-film multilayer model or with the analogue of the Bragg's law in crystallography (DURRER, 1962; LAND, 1972). Although these models effectively introduce optical interference and offer the qualitative explanation for the color, they give the reflective properties considerably different from that of the actual bird feathers: the incident light is reflected to the direction of reflection like a flat mirror in these models, whereas the diffuse reflection is usually observed. Therefore, some additional factors are necessary in order to explain the characteristics of the reflection in real bird feathers.

In the present paper, we report the detailed investigations on the structural and reflective properties of peacock feathers. In particular, the reflection is carefully characterized by observing the angular dependence and also the dependence upon the illuminated area. We show both the submicron regular structure of melanin granules and macroscopic shape/configuration of barbules contribute to the essential part of the iridescent color in peacock feathers.

2. Experimental

A peacock has several kinds of differently colored feathers. Although the most famous one is the uppertail covert of a beautiful eye-pattern, we have chosen brilliant blue feathers covering the major part of the body and yellow feathers under the uppertail coverts to perform the comparative studies on the iridescent colors. These feathers were observed with an optical microscope (Olympus BX50), a scanning electron microscope (SEM, JEOL JSM-5800) and a transmission electron microscope (TEM, JEOL JEM-1200 EX). The samples for the SEM observation were sputtered with gold. The TEM samples were prepared according to the conventional method (SATO *et al.*, 1997). The optical reflection was characterized by the following methods. 1) The angular dependence of the reflected light intensity was measured under monochromatic light illumination by placing one end of an optical fiber on a rotating stage near the sample, while the other end was put in front of a photomultiplier. 2) The angular dependence of the reflected light was spectrally analyzed by a spectrometer (Ocean Optics USB2000) under the illumination of a tungsten lamp or a Xenon lamp. 3) The laser speckle pattern was observed by the use of an Ar-ion laser (Spectra Physics Model 2016) of 488.0 or 514.5 nm. The laser beam was expanded into typically 10 mm in diameter and focused into the sample with a camera lens (Nikon lens series E f35). The beam waist was estimated at about 3 μm under the assumption of the Gaussian profile of the laser beam with an ideal focusing lens. The optical transmission was also measured by using a He-Ne laser of 633 nm with the same focusing system as described above. The transmitted light through a single barbule was detected by a photodiode having a large detection area of 6 mm \times 6 mm, which was placed closely behind the sample.

3. Experimental Results

3.1. Structural observation

We have first observed the surface of a feather with the SEM and the optical microscope. A barb of a feather has a lot of branches called barbules (Fig. 1A). They are

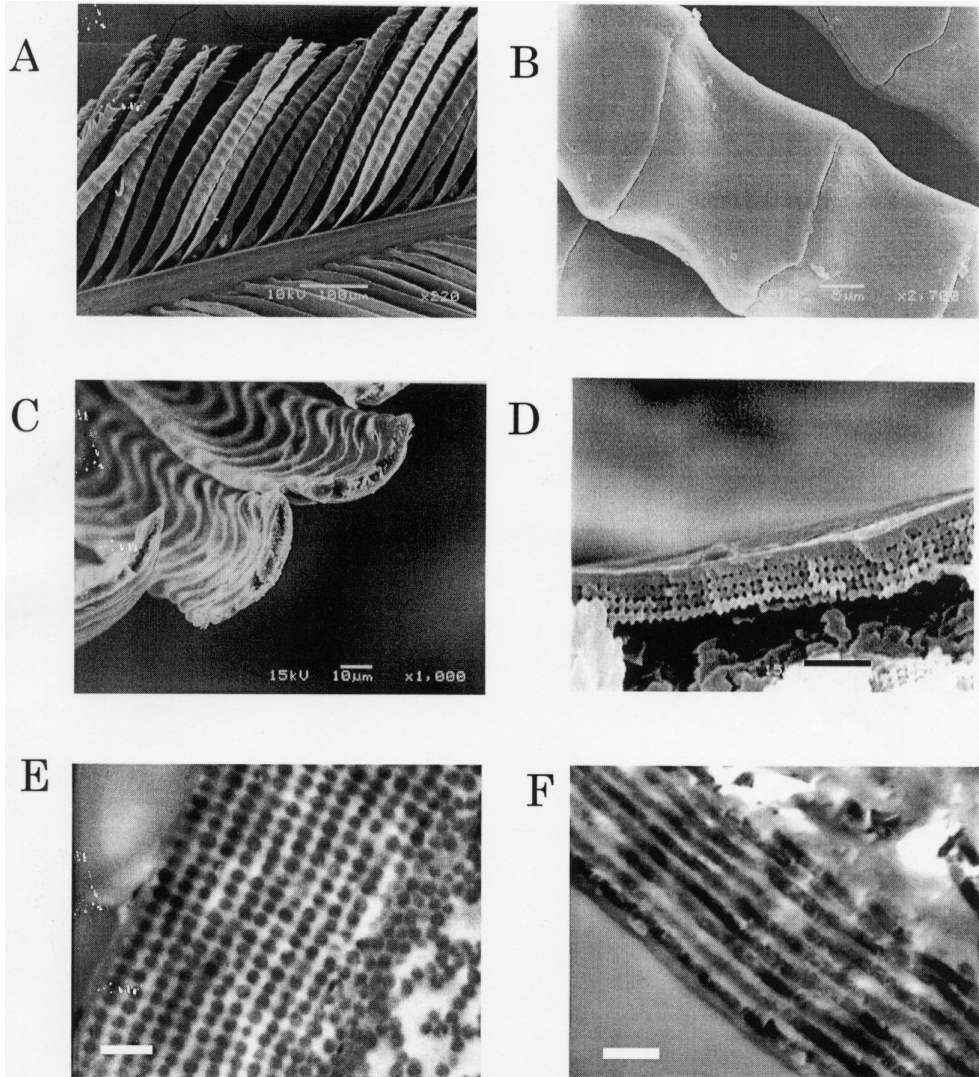


Fig. 1. Scanning and transmission electron microscope images of the iridescent peacock feathers: A) a barb with a lot of barbules of a blue feather, B) several blocks within a barbule of a blue feather, C) the transverse cross section of barbules of a blue feather, D) the transverse cross section of a barbule of a yellow feather observed under higher magnification, E) TEM image of the transverse cross section of a blue feather, F) the longitudinal cross section along a barbule axis for a blue feather. The scale bar is $1 \mu\text{m}$ for D) and 400 nm for E) and F).

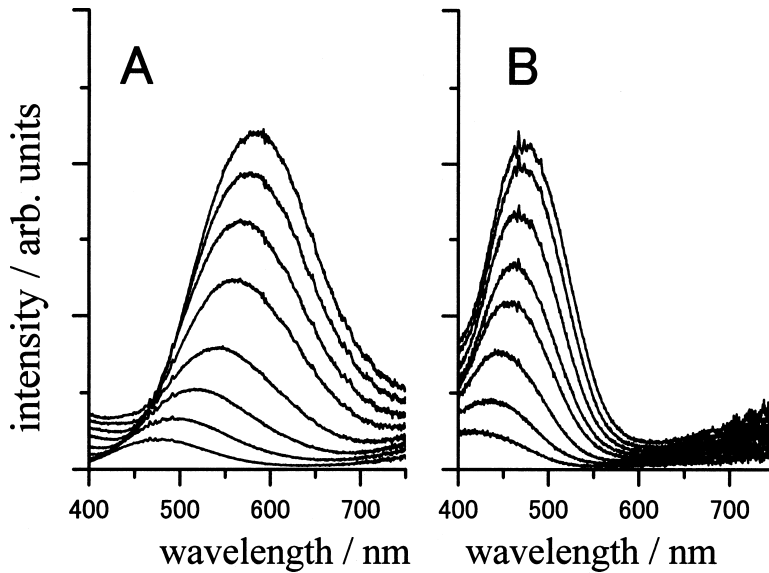


Fig. 2. Angular dependence of the reflection spectrum from several barbs containing a lot of barbules for (A) a yellow feather and (B) a blue feather. The incident angle, which is defined as 0° , is roughly normal to the vane. The observation angles are, from top to bottom, 15° , 25° , 35° , 45° , 55° , 65° , 75° and 85° for (A) and (B).

curved along its long axis and slightly twisted from its root. Further, each barbule has the shape of connected blocks of typically $20\text{--}30\ \mu\text{m}$ (Fig. 1B). It is also found the surface of a block is smoothly curved like a saddle. Actually, a transverse cross section is crescent-shaped as shown in Fig. 1C. From the optical microscope observation, it is confirmed that the brilliant color owes mostly to the blocks of barbule.

Next we have investigated the submicron structure in feathers under a higher magnification. In the transverse cross section of a barbule of a yellow feather, several layers consisting of periodically arrayed particles are observed beneath the surface layer (Fig. 1D). The TEM image more clearly shows the lattice structure of the particles for a blue feather (Fig. 1E). The diameter of a particle is estimated at 130 and 140 nm for blue and yellow feathers, respectively, under the assumption that the particles are close-packed parallel to the surface. It is also noticed that blue and yellow feathers have 8–12 and 3–6 regular layers with the layer intervals of 150 and 190 nm, respectively. Below the lattice structure, the particles are randomly distributed. In contrast to the transverse cross section, the particle has a long shape up to several microns in the longitudinal cross section (Fig. 1F). The regularity of the arrangement along this direction is not observed (DURRER, 1962). These small particles have been thought to be melanin granules and that is consistent with the fact that the barbules of both feathers looks dark brown under the observation of the transmission optical microscope.

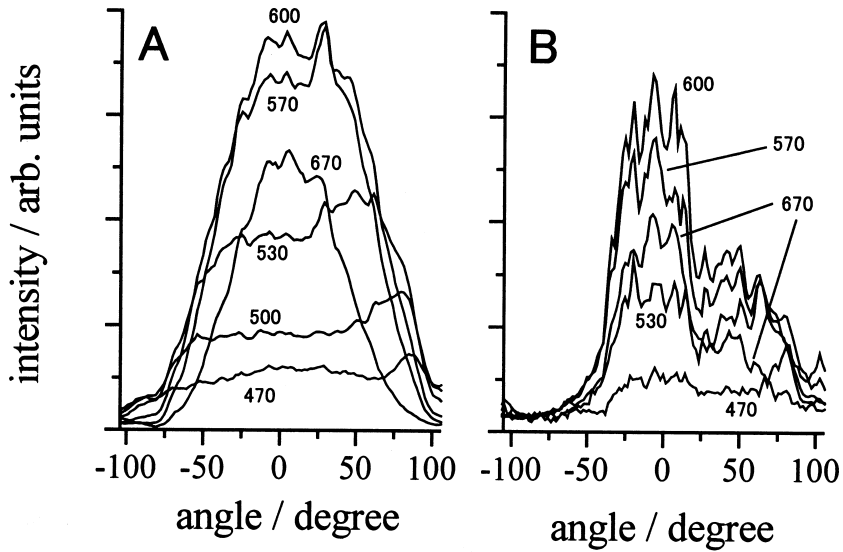


Fig. 3. Angular dependence of the reflected light intensity from (A) a barb with barbules and (B) a single barbule of a yellow feather. The intensity was measured in the plane vertical to the barb in (A) and to the barbule axis in (B) under the roughly normal incidence.

3.2. Reflection properties

We have quantified the iridescence by measuring the angular dependence of the reflection spectrum from several barbules containing a lot of barbules. Figures 2A and 2B show the experimental results for yellow and blue feathers, respectively. The peak position of the spectrum smoothly shifts to shorter wavelength with lowering its intensity as the view-angle is increased, and this behavior is consistent with our visual observation of the iridescent color. The difference between yellow and blue feathers appears not only in the spectral peak position but also in the width of the peak. Namely, the FWHM of ~170 nm for the yellow feather is wider than that of 110 nm for the blue feather. The reflection intensity is also characterized in the angle-resolved experiments. Figure 3A shows the results for barbules in a barb of a yellow feather. It is found that the intensity has a peak roughly at 0° , the direction of incidence, for longer wavelengths from 570 to 670 nm. On the other hand, for shorter wavelengths, the intensity tends to be relatively strong at the largely oblique direction, although the asymmetry of the shape is not reproducible in the different samples.

Next, we show the angular reflectance from a single barbule in Fig. 3B. As is immediately noticed, the behaviors are markedly different from the case of barbules: the curves exhibit irregular peaks at various angles for all the wavelengths investigated. This irregular character is observed for all the barbules examined, although the detailed structures are changeable.

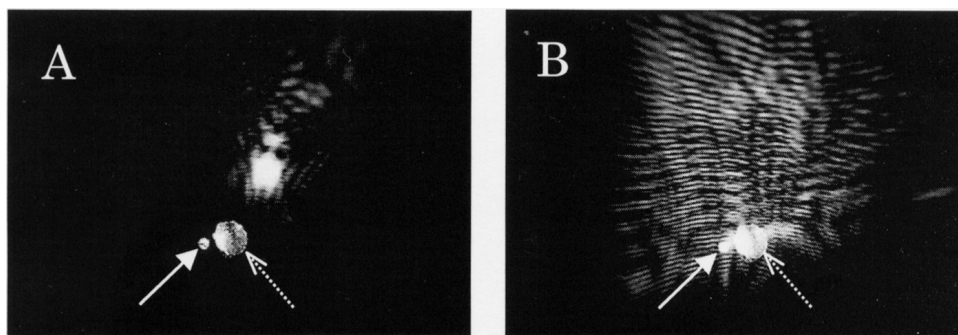


Fig. 4. The laser speckle pattern from a small part within a single barbule observed with the wavelength of 488 nm. The sample is attached to the needle tip and placed vertically at the focal position (A) and at the slightly defocused position (B). The screen was put 3 cm away from the sample. The arrow shows the sample and the broken arrow shows the hole through which the laser beam irradiates the sample.

We further examine a much smaller part of a barbule by employing a laser as a light source and a camera lens for focusing the laser beam. Figures 4A and 4B show the laser speckle patterns obtained by illuminating a small part in a block within a barbule. It is found that the pattern strongly depends on the area of the illumination. When we put the sample at the focal position, namely several μm^2 is illuminated, the reflection is limited within a narrow angular range of typically $20\text{--}30^\circ$ and forms a bright spot of the reflected light (Fig. 4A). On the other hand, the reflected light spreads into a wide angular range when the whole width of the barbule is illuminated as shown in Fig. 4B. It is found that the angular distribution extends up to $80\text{--}120^\circ$ vertically and horizontally. Further, it is noticed that the speckles have a horizontally long shape. These characteristics in the laser speckle are common in both blue and yellow feathers.

4. Discussion

4.1. Submicron structure and optical interference

As Newton pointed out in the 18th century (NEWTON, 1730), the iridescent color strongly suggests the presence of optical interference in peacock feathers. As is observed in the electron microscope images, the regular lattice of the melanin granules seems responsible for optical interference. It is also evident, however, that a simple lattice model fails to explain the reflection in a widely spread angular range as observed in the optical measurements. To reconcile these facts, we consider a new model which introduces the effect of a macroscopic structure in a statistical way in addition to the submicron regular lattice. In this subsection, we clarify how the feather colors are produced by the array of the melanin rods by considering optical interference among the structure. Then, the effect of the macroscopic structure will be introduced to explain the reflective properties in the following subsection.

As a model for the array of the melanin granules, we consider the interaction of the two-dimensional lattice of infinitely long rods with light. The reflection from the model is

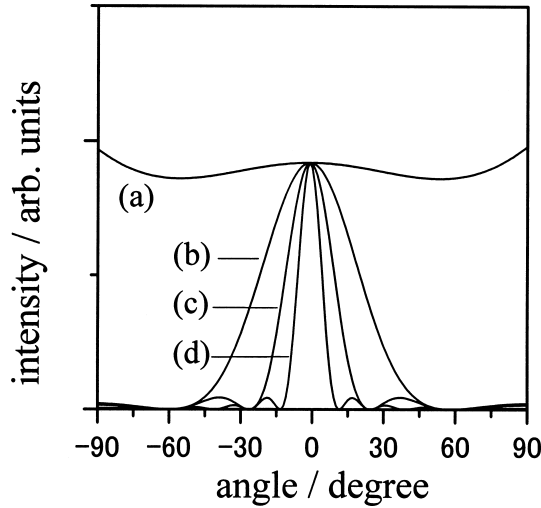


Fig. 5. The angular dependence of the reflection intensity calculated for a single and one-dimensional array of infinitely long rods under the normal incidence. The number of the rods is (a) 1, (b) 5, (c) 10 and (d) 20. The scattered wave from a single rod is approximated by the first three terms of Eq. (1) and the following parameters are used in the calculation: the rod radius of 70 nm, the rod interval of 140 nm, wavelength of 600 nm and the refractive index of 2.0. Intensities are normalized at 0° .

limited within the plane perpendicular to the rods when light is incident normal to the lattice. Before treating the two-dimensional lattice directly, it is helpful to consider first the scattering problem of a plane wave by a single rod. The rigorous solution of Maxwell's equations for an infinitely long rod has been already known for the arbitrary radius of the rod a and the wavelength of the incident wave λ . The field of the scattered wave u_s is expressed as the infinite series including Hankel functions (VAN DE HULST, 1957). In the far field, the asymptotic expression is given as

$$u_s(r, \theta) \sim \sqrt{\frac{2}{\pi kr}} \left(b_0 + 2 \sum_{n=1}^{\infty} b_n \cos n\theta \right), \quad (1)$$

where r is the distance from the rod, θ is defined as the angle between the directions of the incidence and the observation, $k = 2\pi/\lambda$ the wavevector and b_n the coefficients including k , a and the refractive index of the rod. In the above expression, we omit the phase factor for simplicity. When the radius of the rod is smaller than the wavelength of light, the first several terms become dominant in the series. Actually, using the radius of 70 nm and the wavelength of visible light, we can show that the first three terms approximate the series fairly well. Figure 5(a) show an example of the angular dependence of the intensity of the scattered wave in the range of reflection, i.e. backward scattering, for the case the incident wave is unpolarized. The angular dependence is found almost constant, although the

intensity is slightly stronger around the angle of $\pm 90^\circ$ owing to higher scattering efficiency in forward direction.

Next, we consider the optical interference among one-dimensionally arrayed rods parallel to the surface in the transverse cross section. The rod spacing of 140 nm is by far smaller than the visible wavelength. Thus, the first- and higher-order diffraction spots do not appear for the visible light. Moreover, the angular spread of the scattering wave is suppressed as the result of the destructive interference owing to the flatness of the array. In Fig. 5, we show this effect by a simple simulation where light is incident perpendicularly on the regular array of rods. The reflection intensity is calculated by adding the amplitude of each scattered wave with the phase factor in the Fraunhofer region under the assumption that the multiple reflection within the structure is ignored. It is found that the diffraction is considerably suppressed at oblique angles and is limited in a narrower angular range around 0° as the array size becomes larger. This may explain the experimental result shown in Fig. 4A, where we observe the reflection of a bright spot. In fact, it is confirmed that typically more than 10 rods seem to be regularly arrayed in Fig. 1E. Thus, the one-dimensional array of the particles reflects light to a very narrower angular range just like a flat mirror. In other words, the particle array can be regarded as a single uniform layer. We note the spot in Fig. 4A has the angular range of the reflection slightly wider than the converging angle of the laser beam of 16° , which is geometrically determined by the beam diameter and focal length. This difference can be explained by the remaining diffraction effect discussed above and also by the surface curvature, which is discussed in the following section.

Then, the two-dimensionally arrayed rods can be considered as an extension of the above discussion: each array plays a role of a layer and the total system behaves as a multilayer. From the electron microscope observation, the optical path lengths of the round trip amount to 504 and 600 nm for blue and yellow feathers, respectively, which are comparable with the spectral peak positions in Figs. 2A and 2B. These path lengths are calculated using the mean refractive index, which is the spatial average of the indices of 1.0 for air and 2.0 for melanin granule assuming only the real part (LAND, 1972).

4.2. *Effect of macroscopic structure*

Although the multilayer system successfully explains the color of feathers, it does not predict the reflection in a wide angular range. Here we discuss the effect of the macroscopic structure in order to explain this character of the reflection. By the consideration of the large difference observed in the laser speckle patterns for two focusing conditions, it is suggested that the smoothly curved surface is related to the angular dependence of the reflection. Actually, the crescent shape in the transverse cross section causes the tilt of the multilayer to the incident light which results in the spread of the reflection in the plane perpendicular to the barbule axis. Besides, any microscopic imperfections such as the irregular position of the rod and distortion of the shape may contribute to the diffraction of scattered light. Anyway, the surface curvature contributes significantly to the iridescence of the feather color, because the optical path length for the interference becomes shorter when a plane wave is incident obliquely on a multilayer. Similarly, in the longitudinal plane, the origin of the spreading reflection is due to the surface curvature of the barbule along the longitudinal direction, and also to the finite length and the randomly positioned

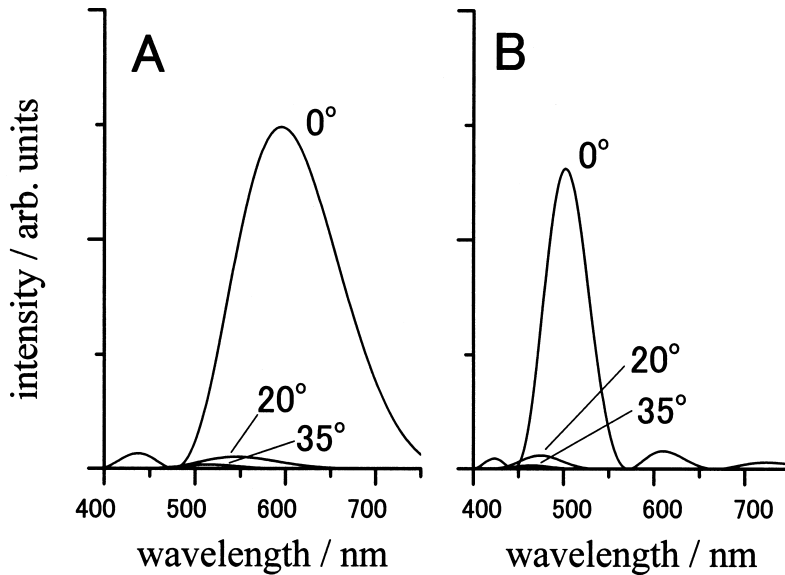


Fig. 6. The calculated reflection spectra at several observation angles by using the model of the two-dimensional lattice of the infinitely long rods. The lattice sizes are 15 parallel to the surface by 4 in depth for (A) and 15 by 8 for (B) with the lattice intervals 300 and 252 nm in the depth direction, respectively. Other parameters are the same as in Fig. 5.

end of the rod. The horizontally long shape of the speckle may reflect the anisotropy of the melanin granules. However, further studies are necessary to explain quantitatively the characteristic pattern.

Let us now focus our attention to further larger structure. As shown in Figs. 3A and 3B, the irregular peaks observed for a single barbule are smoothed, when we observe the reflection from a lot of barbules at a time. It should come from the average over the distribution of the tilt angle of a multilayer. Several factors may contribute to the distribution; 1) the curvature along the barbule axis, 2) the twist of a barbule, and 3) the distribution of the orientation of barbule axis. Although these factors are difficult to treat quantitatively, the experimental results suggest that the macroscopic shape and the configuration of barbules statistically contribute to the smoothly and widely spreading reflection.

4.3. Simulation of the iridescence

Now we will reproduce quantitatively the iridescence of a peacock feather by using the model of two-dimensional lattice of infinitely long rods taking into account the effect of the macroscopic structures. The interaction of the lattice with the incident plane wave is treated as follows:

1) The scattering from a single rod is approximated by the first three terms of the infinite series of the rigorous solution.

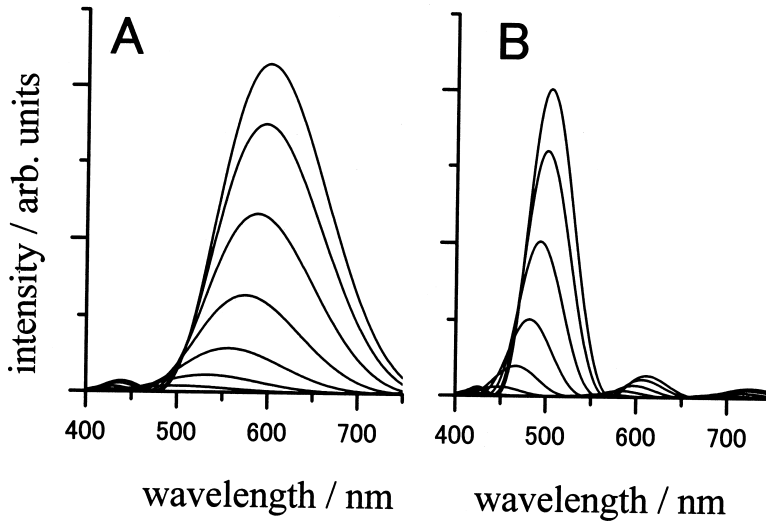


Fig. 7. Angular dependence of the reflection spectra calculated from the model with the distribution of the tilt angle. The distribution function is assumed as a Gaussian function $\exp(-\theta_i^2/\theta_0^2)$ for the tilt angle θ_i and $\theta_0 = 15^\circ$. The observation angles are, from top to bottom, 5° , 15° , 25° , 35° , 45° , 55° and 65° for (A), and 5° , 15° , 25° , 35° , 45° and 55° for (B). The other parameters in the calculation are the same as in Fig. 6.

2) It is assumed that amplitude and phase of the incident wave is not influenced by the scattering at the rods and the scattered wave from a certain rod is not subject to scattering at the other rods.

3) The optical interference among the scattered waves from each rod is considered in the Fraunhofer region.

This treatment gives the field corresponding to the first-order solution of the wave equation under the presence of the dielectric material (KINOSHITA *et al.*, 2002b). First, we show the reflection spectra calculated without the tilt of the lattice for several observation angles in the plane perpendicular to the lattice in Figs. 6A and 6B, where two finite lattices having different dimensions are examined for yellow and blue feathers. The lattice sizes are 15 by 4 and 15 by 8 for the directions parallel to the surface and depth. We decide these dimensions as they correspond to the actual size of the region where the rods are arrayed without imperfection. In the depth direction, the lattice sizes are adjusted to the layer number of each feather with the interval of the optical path length of 300 and 252 nm for yellow and blue feathers, respectively, which is the half of the calculated value for the round trip. As shown in Figs. 6A and 6B, the reflectance has the maximum at the wavelength corresponding to the optical path length of the round trip and successfully explains the feather colors. However, owing to the flatness of the lattice, the angular dependence is extremely different from the experimental results. That is, the intensities suddenly go down as the view angle increased.

Then, we introduce the distribution of the tilt angle of the lattice resulting from the macroscopic shape and configuration of barbules. The distribution is treated by imposing

the statistical weight assumed as a Gaussian function of $\exp(-\theta_i^2/\theta_0^2)$ for the tilt angle θ_i and $\theta_0 = 15^\circ$. The angle θ_0 is determined to reproduce the angular distribution of the experimental results. The value of 15° seems reasonable to characterize the distribution because the tilt angle up to $\pm 30^\circ$ is observed for the crescent shape in Fig. 1C. Thus, Figs. 7A and 7B show the angular dependence of the calculated spectra for yellow and blue feathers, respectively. The line shape and the variation with the observation angle are moderately reproduced on the whole. In this calculation, the spectrum at the observation angle θ mainly comes from the multilayer tilted with the angle $\theta/2$. Therefore, the bandwidth of the spectrum is dominated by two parameters of the multilayer: one is the peak wavelength itself, which is almost proportional to the bandwidth, and the other is the number of the layer. If the latter becomes larger, the layer interval gives the wavevector of the structure with smaller uncertainty, which results in narrower bandwidth in the reflection. In blue feathers, both factors can contribute to the narrower bandwidth.

4.4. Role of pigment

We have found the submicron structure of melanin granules is the origin of the optical interference. Then, why does a peacock utilize the melanin granules to construct the structure? From the viewpoint of optics, one answer is to reduce the background white light such as transmitted light from the back and randomly scattered light inside the feather. Opal is well-known to exhibit the iridescent color which is produced purely by the periodic structure of the regularly stacked SiO_2 particles of several 100 nm in diameter, where a SiO_2 particle is almost transparent for visible light. However, the color is sometimes inconspicuous due to the background white light, which inevitably results from the random scattering due to the irregularities of the structure. In contrast to opal, the pigment in peacock feathers considerably absorbs the transmitted light. Actually, it has been confirmed by the observation that the transmission through a barbule of blue feather is only about 10% for He-Ne laser of 633 nm. The major part of the rest is thought to be absorbed by pigments because the reflectance is relatively low at that wavelength. Inside a barbule, melanin granules exist as two lattices at the front and back surfaces and are randomly distributed between them (DURRER, 1962). All these granules contribute to the absorption of the transmitted light and to the reduction of the background light.

By using the transmission percentage of 10%, we have roughly estimated that the imaginary part of the refractive index of melanin is on the order of $0.01i$ assuming the pigment is uniformly distributed in a barbule and the transmission loss is entirely due to light absorption. We have checked the effect of the imaginary part upon the scattering process of the rod by substituting the complex refractive index into Eq. (1) and found that the scattering efficiency and its angular dependence are almost unchanged. Then, we have examined the influence on the multilayer interference by using the transfer matrix method (BORN and WOLF, 1975). It is found that the maximum reflectance is slightly lowered by the introduction of absorption. That is because the light is gradually extinguished while it is repeatedly reflected inside the multilayer. Similarly, in the bird feathers, the reflectance may be lowered by light absorption. However, in contrast to the uniform multilayer assumed in the calculation, the irregularity of the actual structure easily randomizes the phase of the light as it is reflected many times. Such light becomes the background light and makes the interference color inconspicuous, if the structure is made of a transparent

material. Thus, the pigmentation is thought to have a role to absorb the randomly scattered light and to make vivid the interference color.

In some *Morpho* butterflies, the pigmentation and the periodic structure are realized separately: pigments exist in the lower part of iridescent scales, whereas the structure is made of transparent cuticle in the upper part (KINOSHITA *et al.*, 2002a, b). From the comparison with these butterflies, it is also possible to say that a peacock efficiently achieves both optical interference and pigmentation by using melanin granules.

5. Conclusions

The physical mechanisms for the structural color of peacock feather are summarized as follows:

- 1) The submicron periodic structure of melanin granules causes the optical interference and produces the resultant color.
- 2) The macroscopic structures are essential to statistically realize the diffuse reflection.
- 3) The absorption of the background light by melanin pigment makes vivid the interference color.

It is worthwhile to note that the *Morpho* butterfly scale has the different mechanism of the diffuse reflection from that in the peacock feathers. On the iridescent *Morpho* scale, the microscopic irregularity of the height of the lamellar structure realizes the diffuse reflection in blue color (KINOSHITA *et al.*, 2002a), whereas a peacock utilizes the macroscopic shape of feathers.

Although the structural color of peacock feather is now explained as we see above, the next question immediately arises: how on earth the submicron structure is constructed in a biological system. It is a problem, of course, in embryology. However, the formation process of such a structure is one of the current topics in photophysics, because the self-organization is powerful method to obtain a photonic crystal. Thus, the structural color is an interesting topic from both physical and biological viewpoints.

The present work is partially supported by the Sumitomo Foundation and Kato Memorial Bioscience Foundation.

REFERENCES

- AUBER, L. (1957) The structure producing "non-iridescent" blue colour in bird feathers, *Proc. Zool. Soc. London*, **129**, 455–486.
- BORN, M. and WOLF, E. (1975) *Principle of Optics*, 5th Ed., Pergamon Press, p. 51.
- DURRER, H. (1962) Schillerfarben beim Pfau (*Pavo cristatus* L.), *Verhandl. Naturf. Ges. Basel*, **73**, 204–224.
- DYCK, J. (1971) Structure and spectral reflectance of green and blue feathers of the rose-faced lovebird (*Agapornis roseicollis*), *Biol. Skr.*, **18**(2), 1–67.
- GREENWALT, C. H., BRANDT, W. and FRIEL, D. D. (1960) Iridescent colors of humming-bird feathers, *J. Opt. Soc. Am.*, **50**, 1005–1013.
- KINOSHITA, S., YOSHIOKA, S. and KAWAGOE, K. (2002a) Mechanisms of structural color in the *Morpho* butterfly: cooperation of regularity and irregularity in an iridescent scale, *Proc. R. Soc. London*, **B269**, 1417–1421.

- KINOSHITA, S., YOSHIOKA, S. FUJII, Y. and OKAMOTO, N. (2002b) Photophysics of structural color in the *Morpho* butterflies, *Forma*, **17**, this issue, 103–121.
- LAND, M. F. (1972) The physics and biology of animal reflectors, *Prog. Biophys. Mol. Biol.*, **24**, 77–106.
- MASON, C. W. (1923a) Structural colors in feathers I, *J. Phys. Chem.*, **27**, 201–251.
- MASON, C. W. (1923b) Structural colors in feathers II, *J. Phys. Chem.*, **27**, 401–447.
- NEWTON, I. (1730) *Opticks*, 4th Ed., reprinted by Dover Publications, NY, p. 252.
- PENDRY, J. B. (1994) Photonic band structures, *J. Mod. Optic.*, **41**, 209–229.
- PRUM, R. O., TORRES, R. H., WILLIAMSON, S. and DYCK, J. (1998) Coherent light scattering by blue feather barbs, *Nature*, **396**, 28–89.
- PRUM, R. O., TORRES, R., WILLIAMSON, S. and DYCK, J. (1999) Two-dimensional Fourier analysis of the spongy medullary keratin of structurally coloured feather barbs, *Proc. R. Soc. London*, **266**, 13–22.
- RUTSCHKE, E. (1966) Die submikroskopische Struktur schillernder Federn von Entenvögeln, *Z. Zellforsch.*, **73**, 432–443.
- SATO, A., TOKUNAGA, F., KAWAMURA, S. and OZAKI, K. (1997) In situ inhibition of vesicle transport and protein processing in the dominant negative Rab1 mutant of *Drosophila*, *J. Cell Science*, **110**, 2943–2953.
- SCHMIDT, W. J. and RUSKA, H. (1962) Über das schillernde Federmelanin bei *Heliangelus* und *Lophophorus*, *Z. Zellforsch.*, **57**, 1–36.
- VAN DE HULST, H. C. (1957) *Light Scattering by Small Particles*, John Wiley & Sons, NY, reprinted by Dover Publications (1981), p. 300.